Expanded View Figures

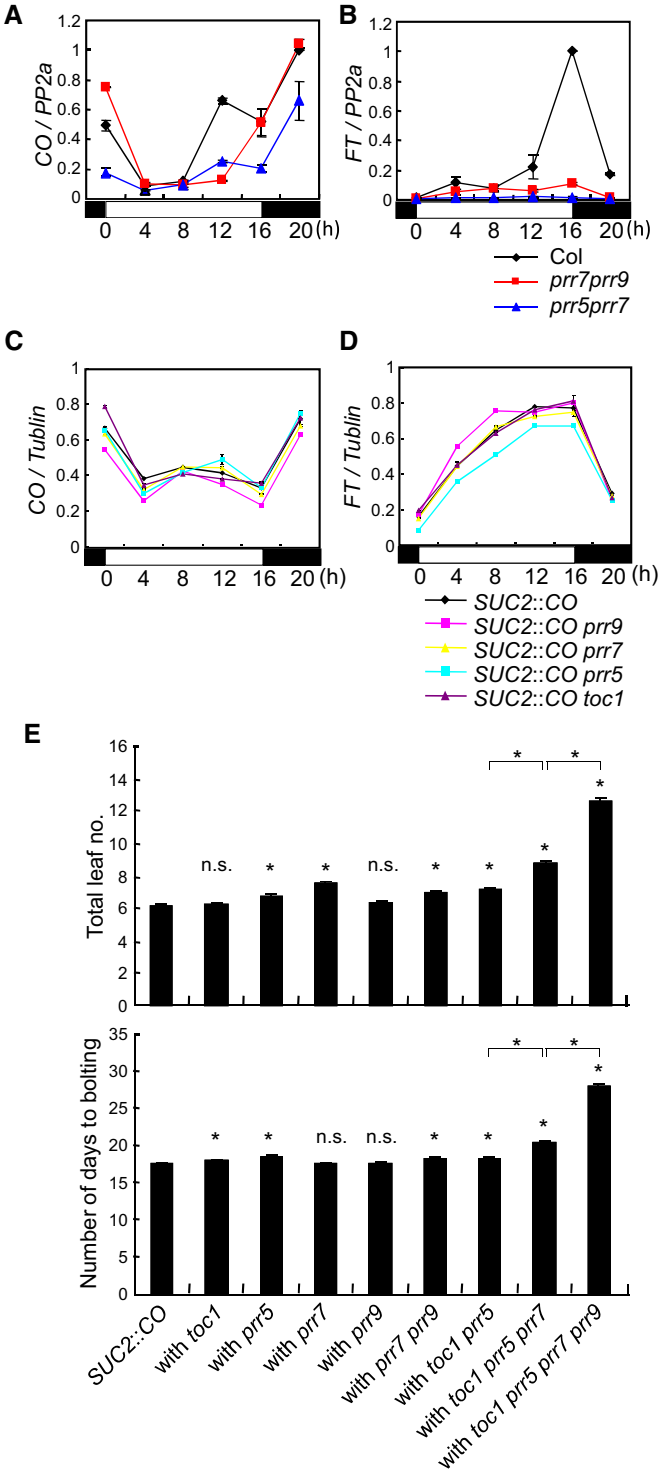

Figure EV1. Effects of *prr* mutations on *FT* expression and flowering time in WT and *SUC2*::*CO* backgrounds.

A, B Expression pattern of *CO* (A) and *FT* (B) mRNA in *prr5 prr7* or *prr7 prr9* double mutants under LD. Error bars indicate standard error within two biological replicates. In each replicate, two technical replicates were performed.

C, D Effect of single *prr* mutations on *CO* (C) and *FT* (D) mRNA accumulation in *SUC2*::*CO* plants under LD. Error bars indicate standard error within two technical replicates.

E Total leaf number and bolting time of *prr* mutants in the *SUC2*::*CO* background grown under LDs. Approximately 40 plants of each genotype were grown under LDs. Error bars indicate standard error. Statistical significance between *SUC2*::*CO* and each *prr* mutant, and among multiple *prr* mutants was calculated using Student's *t*-test; $*P < 0.01$; n.s. $P > 0.01$.

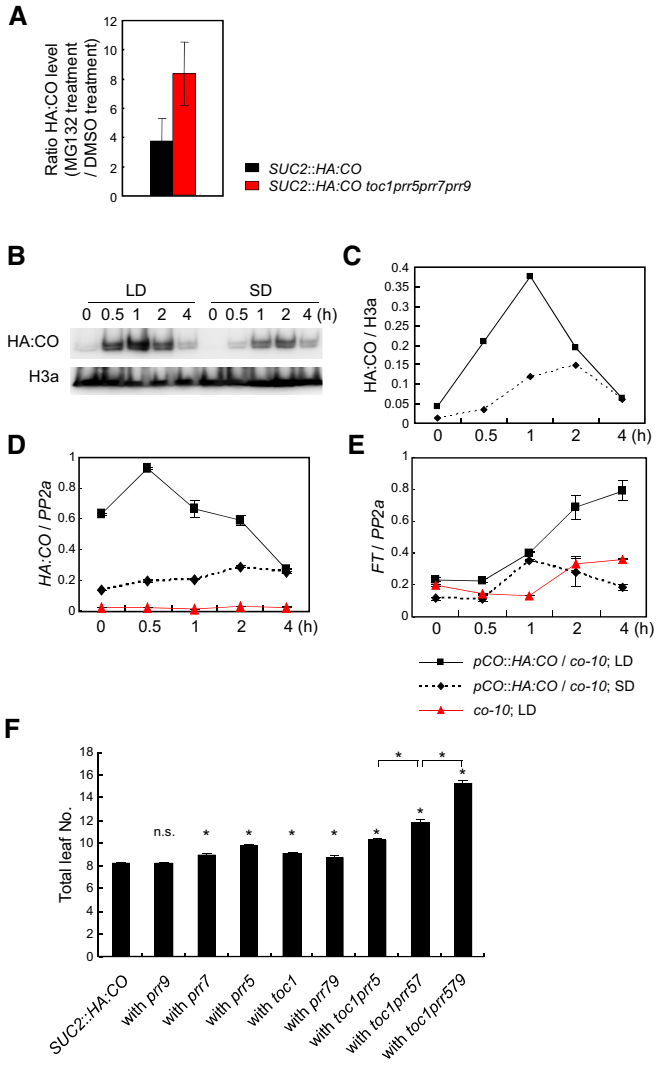

Figure EV2. Stabilization and accumulation of HA:CO through PRR-mediated inhibition of its proteasomal degradation, and its effect on flowering time.

A Effect of MG132 treatment on recovery of HA:CO protein accumulation in *toc1 prr5 prr7 prr9 SUC2::HA:CO*. 10-day-old *SUC2::HA:CO* and *toc1 prr5 prr7 prr9 SUC2::HA:CO* were treated with either MG132 or DMSO at ZT5 and harvested at ZT8 under LD. The levels of HA:CO were normalized to those of H3a. The ratio of the values after MG132 treatment to those after DMSO treatment was calculated in each line, and fold change in HA:CO accumulation by the MG132 treatment was measured. Error bars indicate standard error within two biological replicates. In each replicate, two technical replicates were performed.

B, C Accumulation of HA:CO protein in *pCO::HA:CO* in the morning under LD and SD.

D Accumulation of *HA:CO* mRNA in *pCO::HA:CO* in the morning under LD and SD. Error bars indicate standard error within two technical replicates.

E Accumulation of *FT* mRNA in *pCO::HA:CO* in the morning under LD and SD, and *FT* mRNA accumulation in the morning requires *CO*. Error bars indicate standard error within two technical replicates.

F Total leaf number of *prr* mutants in the *SUC2::HA:CO* background under LDs. 16 plants of each genotype were grown under LDs. Error bars indicate standard error. Statistical significance between *SUC2::HA:CO* and each *prr* mutant, and among multiple *prr* mutants was calculated using Student's *t*-test; $*P < 0.01$; n.s. $P > 0.01$.

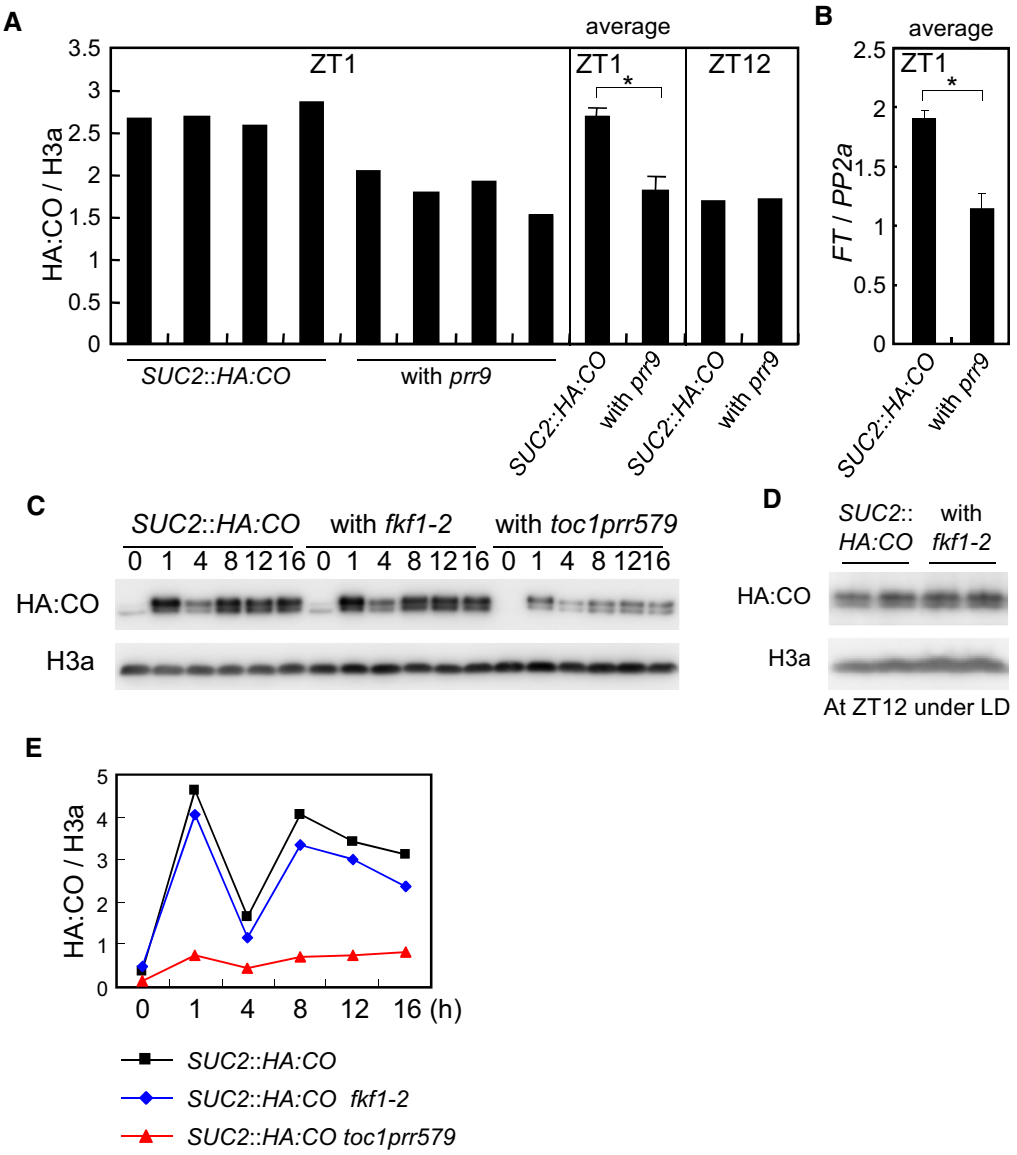

Figure EV3. Effect of *prr9* and *fkf1* mutations on HA:CO accumulation.

A, B Accumulation of HA:CO (A) and *FT* mRNA (B) in *SUC2::HA:CO* and *prr9 SUC2::HA:CO* in the morning. Each genotype was grown in four independent agar plates and harvested at ZT1 under LD. The levels of HA:CO and *FT* mRNA were analyzed in these samples. Error bars indicate standard error within these samples. Statistical significance was calculated using Student's *t*-test, $*P < 0.01$. As the control, HA:CO levels among those lines grown in one plate for each and harvested at ZT12 is shown.

C–E Effect of the *fkf1-2* mutation on HA:CO accumulation in *SUC2::HA:CO* under LD. In (D), each genotype was grown on two independent agar plates and analyzed.

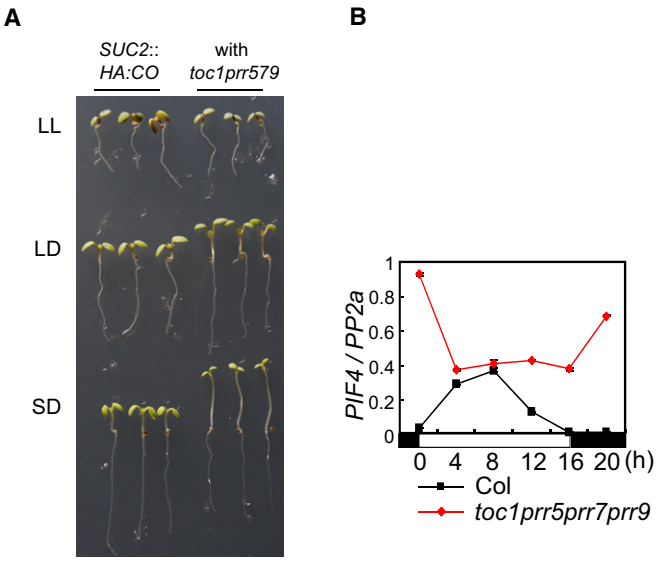

Figure EV4. Hypocotyl growth in the *toc1 prr5 prr7 prr9* mutant under various day lengths and *PIF4* mRNA level in the same background under LD.

A The *prr* quadruple mutant exhibits long-hypocotyl phenotypes under SDs and LDs but not in LL. Plants were grown on agar plates without sucrose for 7 days under LDs, SDs, or LL.

B Transcripts of *PHYTOCHROME INTERACTING FACTOR 4* (*PIF4*) highly accumulate in the *prr* quadruple mutant. Col and *toc1 prr5 prr7 prr9* were grown under LDs. Error bars indicate standard error within two technical replicates.

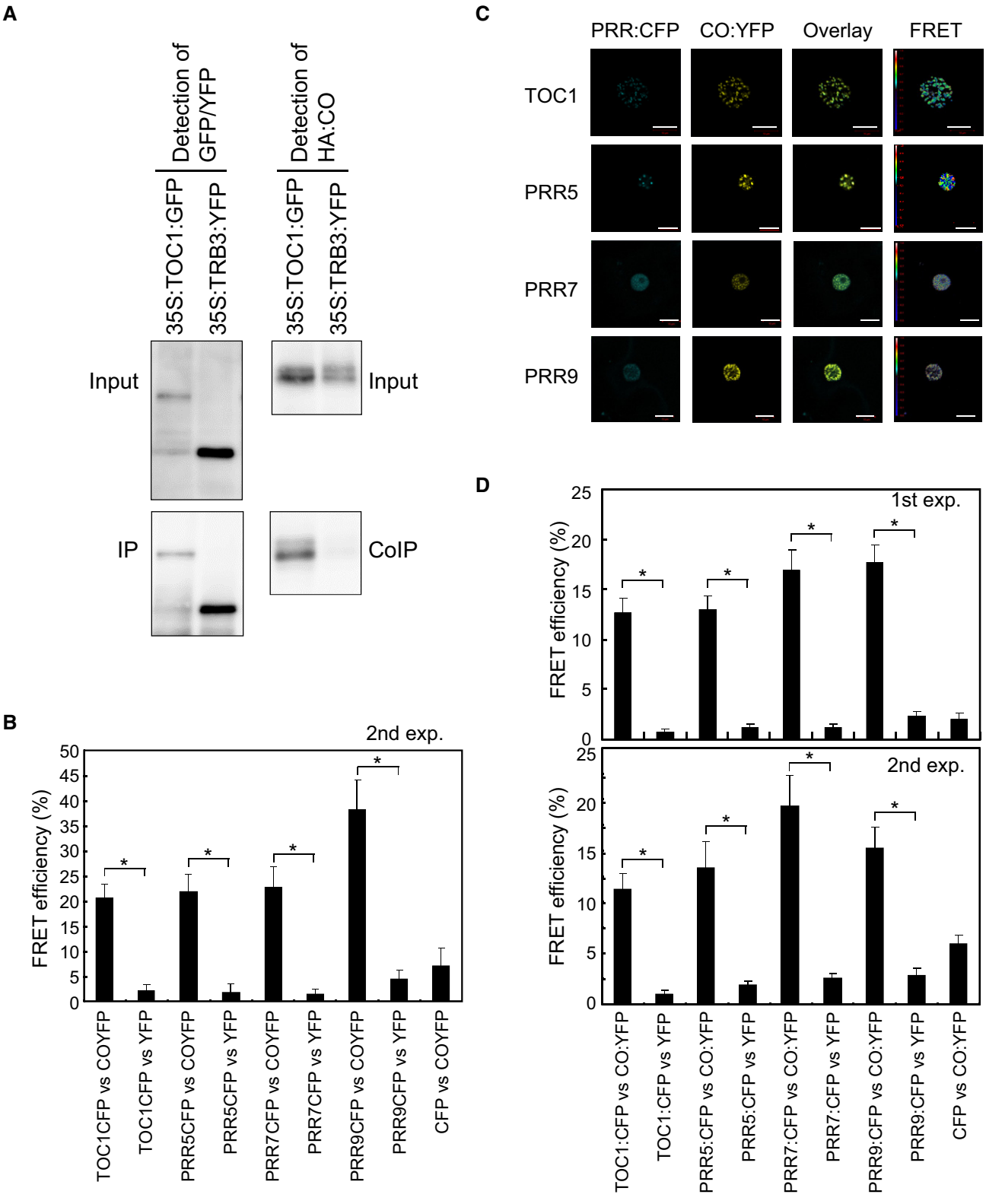

Figure EV5.

Figure EV5. PRRs interact with CO *in vivo*.

A Co-IP experiment in *N. benthamiana*, TRB3 protein was used as the negative control in the experiment shown in Fig 5. *Agrobacterium* carrying either 35S::*TOC1:GFP* or 35S::*TRB3:YFP* were co-infiltrated with that carrying 35S::*HA:CO* in *N. benthamiana* leaves. TOC1:GFP and TRB3:YFP proteins were immunoprecipitated with the GFP antibody, and co-immunoprecipitation of HA:CO protein was checked.

B FRET between PRR:CFP and CO:YFP in *A. thaliana* protoplasts. This is a second experiment of the FRET shown in Fig 5A and B. For each construct combination, FRET in 10 protoplasts was analyzed.

C, D FRET analysis between PRR:CFP and CO:YFP. PRR:CFP and CO:YFP were co-expressed in *N. benthamiana* by Agroinfiltration, and FRET analyses were performed. FRET in 30 cells for each construct combination was analyzed for the first experiment. For the second experiment, 15 cells for each combination were analyzed. Scale bars indicate 10 μm.

Data information: Error bars indicate standard error. In (B) and (D), statistical significance was calculated using Student's *t*-test; $*P < 0.01$.

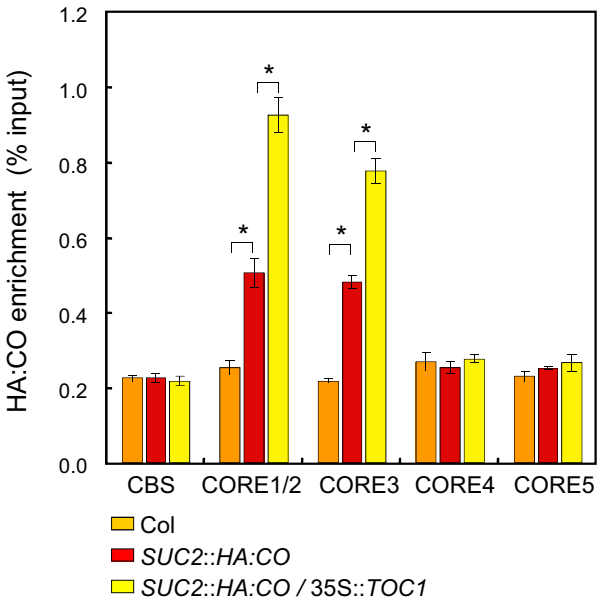

Figure EV6. Overexpression of *TOC1* increases binding of CO to *FT*.
ChIP with 35S::*TOC1 SUC2::HA:CO* at CORE sequences within the *FT* gene. The plants were harvested at ZT12 under LD. HA:CO protein was immunoprecipitated from these lines, and the enrichment of the fragments was measured by qPCR. Error bars indicate standard error among three biological replicates. In each replicate, three technical replicates were performed. Statistical significance differences were obtained with Student's *t*-test, $*P < 0.01$.